





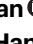

Boreal conifers maintain carbon uptake with warming despite failure to track optimal temperatures

Received: 22 January 2023

Accepted: 13 July 2023

Published online: 03 August 2023

 Check for updates


Mirindi Eric Dusenge ^{1,2,3} , Jeffrey M. Warren ⁴, Peter B. Reich ^{5,6,7}, Eric J. Ward⁸, Bridget K. Murphy ^{3,9,10}, Artur Stefanski ⁵, Raimundo Bermudez⁵, Marisol Cruz ¹¹, David A. McLennan ⁴, Anthony W. King⁴, Rebecca A. Montgomery⁵, Paul J. Hanson ⁴ & Danielle A. Way ^{3,12,13,14} 

Warming shifts the thermal optimum of net photosynthesis (T_{optA}) to higher temperatures. However, our knowledge of this shift is mainly derived from seedlings grown in greenhouses under ambient atmospheric carbon dioxide (CO_2) conditions. It is unclear whether shifts in T_{optA} of field-grown trees will keep pace with the temperatures predicted for the 21st century under elevated atmospheric CO_2 concentrations. Here, using a whole-ecosystem warming controlled experiment under either ambient or elevated CO_2 levels, we show that T_{optA} of mature boreal conifers increased with warming. However, shifts in T_{optA} did not keep pace with warming as T_{optA} only increased by 0.26–0.35 °C per 1 °C of warming. Net photosynthetic rates estimated at the mean growth temperature increased with warming in elevated CO_2 spruce, while remaining constant in ambient CO_2 spruce and in both ambient CO_2 and elevated CO_2 tamarack with warming. Although shifts in T_{optA} of these two species are insufficient to keep pace with warming, these boreal conifers can thermally acclimate photosynthesis to maintain carbon uptake in future air temperatures.

Photosynthesis is the largest annual carbon flux between the atmosphere and the biosphere¹, taking up ~123 gigatons of carbon per year from the atmosphere². Terrestrial photosynthesis is ~11 times higher than annual anthropogenic CO_2 emissions¹, offsetting a significant fraction of anthropogenic CO_2 emissions^{3,4}. Thus, relatively small

changes in terrestrial photosynthesis due to global change drivers, such as warming and drought, could increase the rate of atmospheric CO_2 accumulation and associated climate warming predicted by Terrestrial Biosphere Models (TBMs)⁵ that are a key component of global climate models.

¹Department of Biology, Mount Allison University, Sackville, NB E4L 1E4, Canada. ²Western Centre for Climate Change, Sustainable Livelihoods and Health, Department of Geography and Environment, The University of Western Ontario, London, ON N6G 2V4, Canada. ³Department of Biology, The University of Western Ontario, London, ON N6A 3K7, Canada. ⁴Climate Change Science Institute and Environmental Sciences Division, Oak Ridge National Laboratory, Oak Ridge, TN 37830, USA. ⁵Department of Forest Resources, University of Minnesota, Saint Paul, MN 55108, USA. ⁶Hawkesbury Institute for the Environment, University of Western Sydney, Penrith, NSW 2753, Australia. ⁷Institute for Global Change Biology, and School for the Environment and Sustainability, University of Michigan, Ann Arbor, MI 48109, USA. ⁸US Geological Survey, Wetland and Aquatic Research Center, Lafayette, LA, USA. ⁹Department of Biology, University of Toronto Mississauga, Mississauga, ON L5L 1C6, Canada. ¹⁰Graduate Program in Cell and Systems Biology, University of Toronto, Toronto, ON M5S 3B2, Canada. ¹¹Departamento de Ciencias Biológicas, Universidad de Los Andes, Bogota, Colombia. ¹²Division of Plant Sciences, Research School of Biology, The Australian National University, Canberra, ACT 2601, Australia. ¹³Nicholas School of the Environment, Duke University, Durham, NC 27708, USA. ¹⁴Environmental and Climate Sciences Department, Brookhaven National Laboratory, Upton, NY 11973, USA.

 e-mail: mdusenge@mta.ca; danielle.way@anu.edu.au

To improve predictions of CO₂ exchange between terrestrial vegetation and the atmosphere in the warmer, elevated CO₂ climates of the future, it is critical to account for acclimation of photosynthesis to both warming and elevated CO₂ within TBMs^{6,7}. The photosynthetic temperature sensitivity functions currently employed within TBMs were developed using data largely derived from young trees grown in greenhouse warming experiments under ambient atmospheric CO₂ conditions^{6,8}. Thus, it is unclear whether these thermal responses accurately represent mature trees growing in natural conditions in the field and whether they hold under elevated atmospheric CO₂ conditions.

Photosynthesis is regulated by several types of processes (biochemical, biomechanical and diffusional) which are all temperature dependent^{9–11}. In the short-term (minutes to hours), photosynthesis responds non-linearly to temperature, increasing up to a thermal optimum (T_{optA}) and decreasing at supra-optimal temperatures. The decrease of photosynthesis at supra-optimal temperatures is caused by various processes including increased membrane fluidity^{12,13}, impaired redox reactions between protein complexes and electron carriers¹⁴, reduced intracellular CO₂ availability due to stomatal closure¹⁵, deactivation of the key photosynthetic enzyme Rubisco (ribulose-1,5-biphosphate carboxylase/oxygenase)¹⁶, and the release of previously-fixed CO₂ through high respiration and photorespiration rates^{5,9–11}. When exposed to long-term warming (days to years), plants generally acclimate photosynthesis by increasing the T_{optA} ^{8,11,17–23}, thereby increasing net carbon uptake at the new warmer temperature. This acclimation to high temperatures can involve decreased thylakoid membrane fluidity²⁴, expression of a more heat-stable Rubisco²⁵ and Rubisco activase¹¹, expression of heat shock proteins¹¹, and decreases in respiration^{26–28}. However plants differ greatly in their ability to thermally acclimate T_{optA} , with reported values in the literature ranging from increases in the T_{optA} of 0.16–0.78 °C per 1 °C of warming^{8,11,19,22,29–31}. Among the conifers that dominate the boreal forest, some species have shown the ability to acclimate T_{optA} ^{30,32,33} to warming, while others have not³⁴. Whether such stark differences in acclimation capacity are truly representative (i.e., do some species acclimate while others do not) or result from modest sampling intensity is as of yet unclear. Moreover, these studies on boreal conifers have been conducted on seedlings in growth chambers and greenhouses, and it is unclear whether these photosynthetic acclimation responses translate to mature trees growing in the variable air temperatures found in the forest. Furthermore, these studies rarely investigate whether increases in T_{optA} match increases in growth temperature. In a three-year field warming study on broad-leaved boreal and temperate seedlings, shifts in T_{optA} occurred but were much smaller than increases in growth temperatures¹⁹. However, no study to date has explored whether mature field-grown conifers, the trees that represent the majority of the boreal forest, can adjust T_{optA} to compensate for the increasing air temperatures expected over the next few decades.

Photosynthesis and T_{optA} are also affected by elevated CO₂. Elevated CO₂ concentrations stimulate photosynthesis because CO₂ is the substrate for Rubisco^{35–37}, the carboxylating enzyme in C₃ photosynthesis. In the long term, this initial stimulation of photosynthesis often (but not always³⁸) diminishes³⁹ due to acclimation of the photosynthetic biochemistry to elevated CO₂ concentrations and plant sink limitations^{36,40,41}. In some instances, the initial stimulation of photosynthesis by high CO₂ completely disappears, mainly due to nitrogen limitation⁴². By increasing the concentration of CO₂ around Rubisco, growth in elevated CO₂ concentrations also suppresses photorespiration⁴³, a process that releases previously fixed CO₂. Given that high temperatures stimulate photorespiration^{5,9,44}, plants grown and measured under elevated CO₂ have a higher T_{optA} than those grown and measured at current CO₂ levels^{9,18,23,30}, reflecting the suppression of photorespiration at high temperatures by elevated CO₂^{9,30,45}.

Studies of the thermal sensitivity of photosynthesis have focused on ambient CO₂-grown plants^{5,8,11,17,20,46}, and less on how elevated CO₂ may alter temperature acclimation^{5,47}. Because of this, the temperature sensitivity functions currently employed in TBMs are derived from ambient CO₂-grown plants^{6,48}. To date, only a handful of studies have assessed the effect of elevated CO₂ on thermal acclimation of photosynthesis^{23,30}, and only one has investigated the effect of elevated [CO₂] on the temperature sensitivity parameters of net photosynthesis and its underlying biochemical processes (maximum Rubisco carboxylation rate— V_{cmax} , and maximum electron transport rates— J_{max})³⁰. This latter study, conducted on boreal conifer seedlings grown in pots for six months, reported that elevated CO₂ had little effect on thermal acclimation of the temperature sensitivity parameters of V_{cmax} and J_{max} (i.e., their thermal optima and activation energies)³⁰. In the same study, warming increased T_{optA} by 0.36–0.65 °C per 1 °C warming regardless of CO₂ treatments. But elevated CO₂-grown seedlings had a T_{optA} that was generally 3.6–4 °C higher than their ambient CO₂-grown counterparts when measured at prevailing growth CO₂, likely due to direct suppression of photorespiration by elevated CO₂.

The key photosynthetic temperature sensitivity parameters employed in TBMs include T_{optA} , as well as the thermal optima (T_{optV} and T_{optJ}) and activation energies (E_{aV} and E_{aJ}) of V_{cmax} and J_{max} ^{6,7}. The responses of these parameters to long-term changes in temperature, either due to experimental warming or natural seasonal variation, are primarily driven by thermal acclimation and less influenced by adaptation to different thermal environments^{8,21}. This implies that results generated in this study, using boreal tree species, could have implications for plants grown in natural conditions from different thermal environments.

In this study, we assessed the thermal acclimation of photosynthesis and its underlying biochemical processes (i.e., V_{cmax} and J_{max}) in mature trees (~45 years) of tamarack (also known as larch), a deciduous conifer, and black spruce, an evergreen conifer, exposed to either ambient (hereafter aCO₂) or elevated CO₂ (≈+460 ppm above ambient; hereafter eCO₂) combined with a warming of up to +9 °C above ambient temperatures in a regression-based design with five temperature treatments (ambient +0, +2.25, +4.5, +6.75, and +9). The data presented were collected after 2 years of warming combined with one year of CO₂ treatment at the Oak Ridge National Laboratory's SPRUCE (Spruce and Peatland Responses Under Changing Environments; <https://mnspruce.ornl.gov>) project site at the U.S. Forest Service's Marcell Experimental Forest, in Minnesota, USA (47°30.476' N; 93°27.162' W).

Here we show that T_{optA} of mature boreal conifers increased with warming, and this warming-induced increases in T_{optA} were correlated with simultaneous increases of the thermal optima of underlying photosynthetic biochemical processes (V_{cmax} and J_{max}). However, shifts in T_{optA} did not keep pace with warming as T_{optA} only increased by 0.26–0.35 °C per 1 °C of warming. But when estimated at the mean growth temperature, net photosynthetic rates increased with warming in eCO₂ spruce, while remaining constant in aCO₂ spruce and in both aCO₂ and eCO₂ tamarack with warming. Our overall finding is that, although shifts in T_{optA} of these two species are insufficient to keep pace with warming, these boreal conifers can thermally acclimate photosynthesis to maintain carbon uptake in future air temperatures.

Results

Shifts in thermal optimum of net photosynthesis (T_{optA})

The T_{optA} increased by 0.26 and 0.35 °C per 1 °C warming in tamarack and black spruce, respectively, and this shift was similar for both aCO₂- and eCO₂-grown trees (Fig. 1, Supplementary Figs. 1 and 2, and Supplementary Table 1). In addition, T_{optA} was 3 °C higher in eCO₂-grown than ambient-grown tamarack, while CO₂ had no effect on T_{optA} in black spruce (Fig. 1 and Supplementary Table 1). Warming-induced

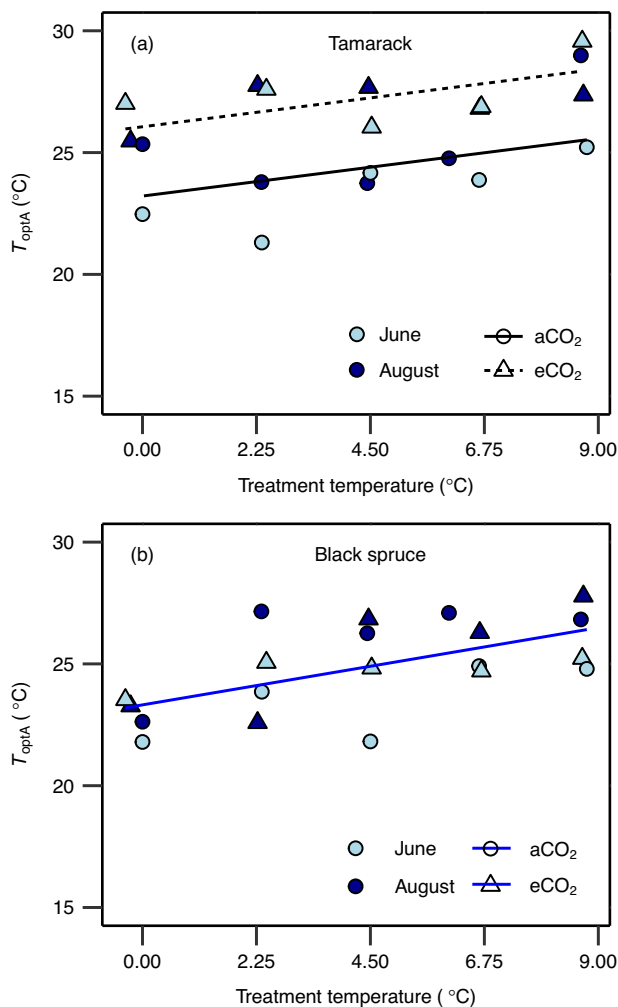


Fig. 1 | Optimum temperature of net photosynthesis across warming and elevated CO₂ treatments. Impact of temperature and CO₂ treatments on the thermal optimum of net photosynthesis (T_{optA} , °C) in tamarack (a) and black spruce (b). The T_{optA} was estimated from temperature response of net photosynthesis measured at growth CO₂ using Eq. 2 (see “Methods”). Symbol colors represent the month in which measurements were taken (June = light blue; August = dark blue). Symbol shapes represent CO₂ treatments (circle = ambient CO₂ – aCO₂; triangles = elevated CO₂ – eCO₂). A mixed-effects regression model was used to analyze the data where warming and elevated CO₂ treatment were the fixed effects, and the month in which the campaign was done was the random effect. The statistical test was one-sided since it was done to evaluate whether warming and elevated CO₂ increase T_{optA} . Lines represent regression lines: in (a) the solid ($y = 0.26x + 23.2$; $p = 0.021$) and the short-dashed ($y = 0.26x + 26$; $p = 0.021$) lines represent ambient and elevated CO₂ treatments, respectively; in (b) the blue line represents the overall regression line when there is no effect of CO₂ on the slope and intercept ($y = 0.35x + 23.3$; $p = 0.0058$). Each data point represents the mean value of biologically independent trees measured in each plot ($n = 1-4$ trees/plot). Significance threshold: $p < 0.05$. Further details on statistical analyses for this figure can be found in Supplementary Table 1.

increases in T_{optA} were correlated with increases of the thermal optima of photosynthetic biochemical processes, T_{optV} (0.35 and 0.44 °C per 1 °C warming for tamarack and black spruce, respectively) and T_{optJ} (0.26 and 0.55 °C per 1 °C warming for tamarack and black spruce, respectively) (Fig. 2, Supplementary Figs. 3–7, and Supplementary Tables 1 and 2). There was no evidence of acclimation of the activation energy for V_{cmax} in either species (Supplementary Fig. 3e, f). However, in black spruce the activation energy of J_{max} declined non-linearly with warming in eCO₂-grown trees but not in aCO₂-grown counterparts,

while in tamarack it was unaffected by warming (Supplementary Figs. 3g, h and Supplementary Tables 1 and 2). Furthermore, neither stomatal conductance nor respiration were correlated with the shifts in T_{optA} seen in either species (Supplementary Table 3a, b).

Exceedance of T_{optA} by mean growth temperature

Photosynthesis typically acclimates to prolonged exposure to warming within 10 days^{19–21}. Therefore, we assessed to what extent warming-induced shifts in T_{optA} matched the increases in growth temperature (expressed as the difference between mean air temperature for the 10 days preceding each measurement and the respective T_{optA} ; $\Delta MeanT_g$). This approach assumes that leaf and air temperatures are similar, a reasonable assumption considering the tight coupling between leaf and air temperature in small leaves⁴⁹, such as conifer needles. In aCO₂-grown tamarack and black spruce, mean daytime growth temperature exceeded T_{optA} ($\Delta MeanT_g > 2$ °C) across all warming treatments (+2.25 to +9 °C) (Fig. 3 and Supplementary Table 4). However, eCO₂ reduced the $\Delta MeanT_g$ for tamarack in the +2.25 °C treatment, while for black spruce, eCO₂ had weak or no effect on $\Delta MeanT_g$ across all warming treatments (Fig. 3b, d and Supplementary Table 4).

Elevated CO₂ impacts on thermal sensitivity of net photosynthesis

We also examined the impact of the treatments on the model parameter representing the spread of the instantaneous temperature response of net photosynthesis (b in Eq. 2, see “Methods”). A high b value represents a narrower temperature response curve of photosynthesis and thus higher sensitivity to short-term temperature fluctuations²¹. In both species, b was unaffected by warming in aCO₂-grown trees. However, the impact of eCO₂ differed between the two species. In tamarack, b was constant in eCO₂-grown trees across the warming treatments, but 86% higher than in the aCO₂ tamarack (Supplementary Fig. 9 and Supplementary Table 1), suggesting an overall CO₂-induced increase in short-term temperature sensitivity (Supplementary Fig. 2). In contrast, in black spruce, CO₂ had no effect on b in the temperature control treatments (+0). However, b marginally increased ($p = 0.067$) with warming in the eCO₂-grown trees, such that it was 68% higher in eCO₂ than in AC in the warmest plot (+9 °C) (Supplementary Fig. 9 and Supplementary Table 1), suggesting an eCO₂-induced increase in the temperature sensitivity of net photosynthesis as it gets warmer (Supplementary Fig. 3).

Net photosynthetic rates at the T_{optA} and growth temperature

Thermal acclimation of net photosynthesis can also be assessed by examining the extent to which net photosynthetic rates at the thermal optimum (A_{opt}) and at prevailing growth temperature are affected by warming¹⁷. In tamarack, A_{opt} was constant across the warming treatments but with overall higher rates in eCO₂ trees compared to their aCO₂ counterparts (Fig. 4a and Supplementary Table 1). By contrast, in black spruce, there was an interaction of warming and elevated CO₂ such that A_{opt} significantly increased with warming in eCO₂ trees, while it was constant across warming in aCO₂ trees (Fig. 4b and Supplementary Table 1). Moreover, net photosynthetic rates estimated at mean (A_g) growth temperature exhibited similar responses to A_{opt} in both species (Fig. 5 and Supplementary Table 1). These results suggest that, overall, the two species were able to maintain their carbon uptake at prevailing growth temperatures. We further estimated net CO₂ assimilation at growth temperature conditions for 2 years (2016 and 2017), representing the entire acclimation period to temperature in this study. The results show that net CO₂ assimilation rates were not negatively affected by warming in either species throughout the growth seasons of both 2016 and 2017. In tamarack, A_g was constant across warming and CO₂ treatments throughout the growth seasons of the 2 years (Supplementary Fig. 10 and Supplementary Table 5).

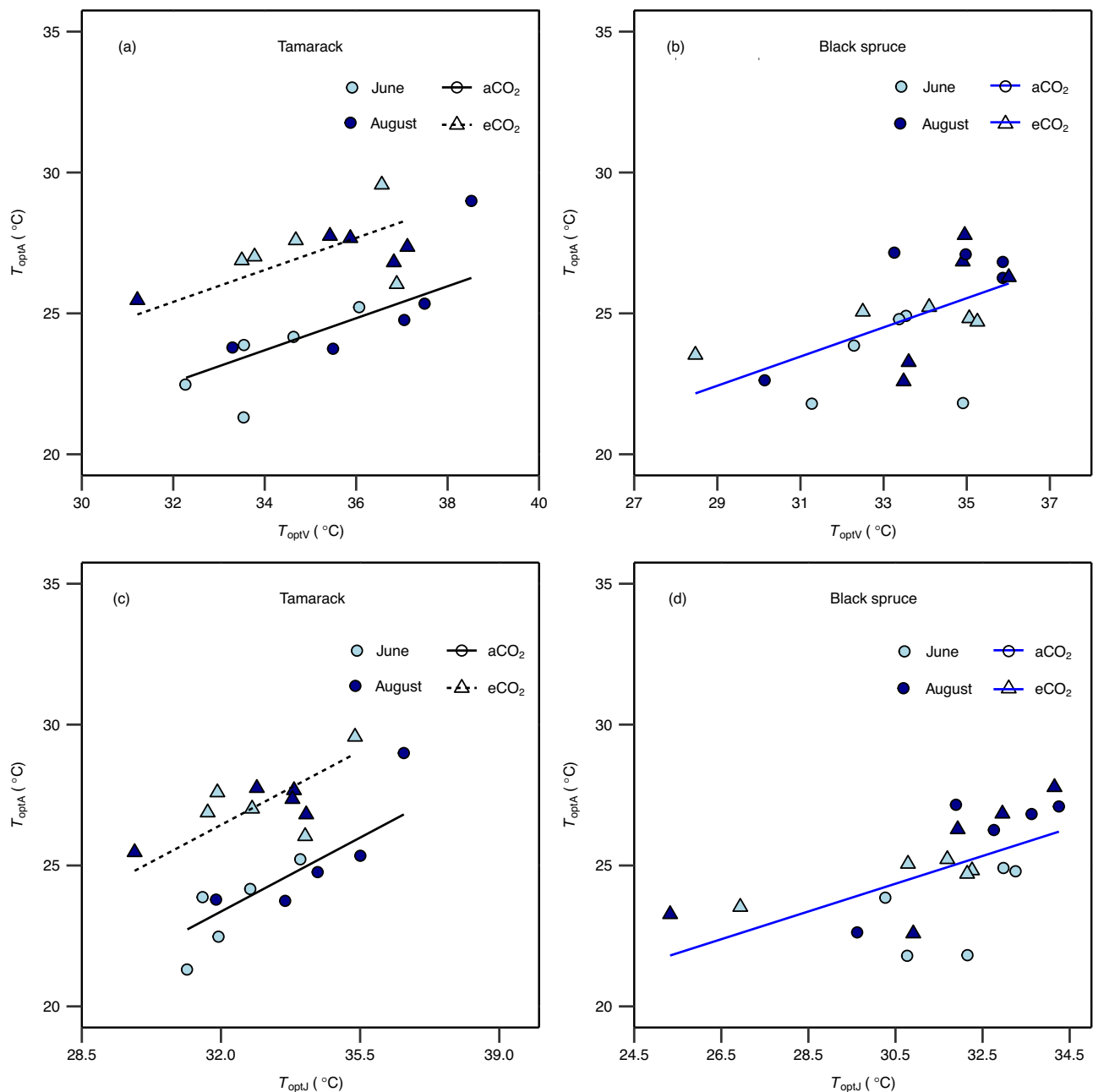


Fig. 2 | Relationship between the optimum temperature of net photosynthesis and the optima temperatures of underlying biochemical processes. The temperature optimum of net photosynthesis measured at growth CO_2 (T_{optA} , °C) as a function of the thermal optimum of **a, b** the maximum Rubisco carboxylation rate (T_{optV} , °C); **c, d** the maximum electron transport rate (T_{optJ} , °C) in tamarack (**a, c**) and black spruce (**b, d**). Symbol colors represent the month in which measurements were taken (June = light blue; August = dark blue). Symbol shapes represent CO_2 treatments (circle = ambient CO_2 — aCO_2 ; triangles = elevated CO_2 — eCO_2). A mixed-effects regression model was used to analyze the data where warming and elevated CO_2 treatment were the fixed effects, and the month in which the campaign was done was the random effect. The statistical test was one-sided since it was done to

evaluate whether there is a positive relationship among the thermal optima of net photosynthesis and underlying biochemical processes. Lines represent regression lines: in (**a, c**) the solid (**a**: $y = 0.57x + 4.4$, $p = 0.0011$; **c**: $y = 0.75x - 0.62$, $p < 0.0001$) and short-dashed (**a**: $y = 0.57x + 7.1$, $p = 0.0011$; **c**: $y = 0.75x + 2.4$, $p < 0.0001$) lines represent ambient and elevated CO_2 treatments, respectively; in (**b, d**) the blue line (**b**: $y = 0.52x + 7.4$, $p = 0.0108$; **d**: $y = 0.56x + 7.3$, $p = 0.0026$) represents overall regression line when there is no effect of CO_2 on the slope and intercept. Each data point represents the mean value of biologically independent trees measured in each plot ($n = 1\text{--}4$ trees/plot). Significance threshold: $p < 0.05$. Further details on statistical analyses for this figure can be found in Supplementary Table 2.

In black spruce, A_g was largely constant across warming treatments in both years for aCO_2 trees, while for eCO_2 trees, A_g commonly increased with warming (Supplementary Fig. 11 and Supplementary Table 5).

Discussion

We report findings, to our knowledge, from the first field study assessing responses of the short-term temperature sensitivity of

photosynthesis to long-term exposure to whole-ecosystem warming (2 years) combined with elevated atmospheric CO_2 (1 year) in mature trees (~45 years old). These results provide a benchmark for our understanding of the impacts of these climate change variables (and their potential interaction) on the thermal sensitivity of photosynthesis in long-lived trees that are experiencing gradual increases in temperature and atmospheric CO_2 in their natural environment.

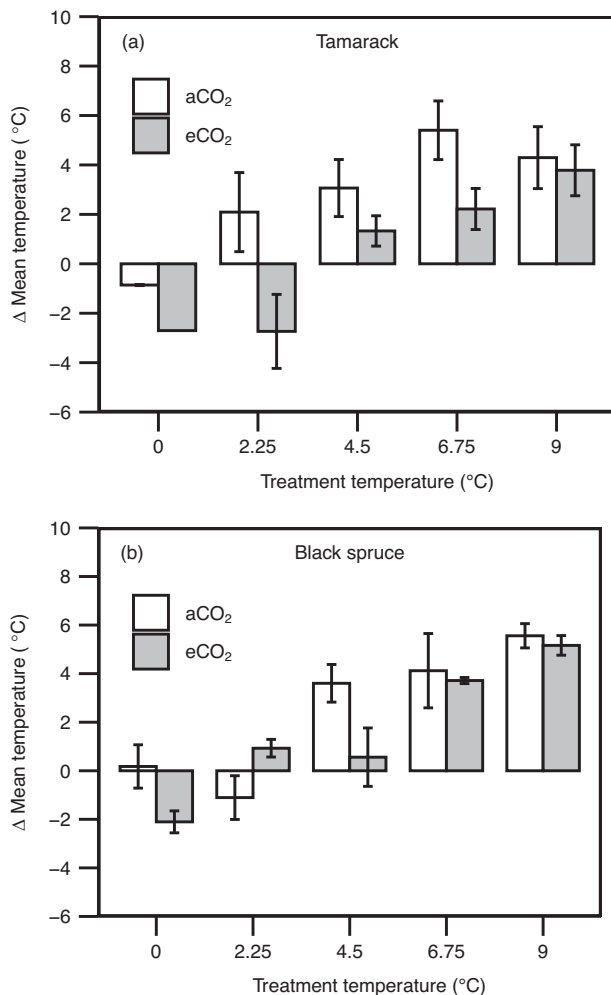


Fig. 3 | Changes in the difference between the optimum temperature of net photosynthesis and prevailing growth temperature across warming and elevated CO₂ treatments. Difference (Δ) between mean daytime (9 am to 3 pm—time of the day when plants are most photosynthetically active) air temperature (°C) and the temperature optimum of net photosynthesis measured at growth CO₂ (T_{optA} , °C) for tamarack (a) and black spruce (b). The mean daytime air temperature corresponded to the average temperature across 10 days prior to each measurement day. Bar colors represent CO₂ treatment (white = ambient CO₂—aCO₂; gray = elevated CO₂—eCO₂). For (a), $n = 2, 1, 3, 3, 2, 3, 3, 3, 3, 3$, and 3 biologically independent trees for +0 aCO₂, +0 eCO₂, +2.25 aCO₂, +2.25 eCO₂, +4.5 aCO₂, +4.5 eCO₂, +6.75 aCO₂, +6.75 eCO₂, +9 aCO₂, and +9 eCO₂ treatments, respectively; for (b), $n = 2, 3, 3, 3, 3, 2, 3, 3, 3, 3$, and 3 biologically independent trees for +0 aCO₂, +0 eCO₂, +2.25 aCO₂, +2.25 eCO₂, +4.5 aCO₂, +4.5 eCO₂, +6.75 aCO₂, +6.75 eCO₂, +9 aCO₂, and +9 eCO₂ treatments, respectively. Mean \pm SE. Further details on statistical analyses for this figure can be found in Supplementary Table 4.

We show that the thermal optimum of net photosynthesis (T_{optA}) increased by 0.26–0.35 °C per °C warming in mature boreal conifers (Fig. 1). These results are comparable to those from a long-term (3 years) field-based warming study with boreal and temperate seedlings, which reported a rise in T_{optA} of -0.38 °C per °C warming¹⁹. However, our T_{optA} values were largely exceeded by mean daytime growth temperature under current atmospheric CO₂ conditions (Fig. 3), suggesting that shifts in T_{optA} in mature trees of boreal conifers growing in the natural field conditions may not fully adjust to compensate for increases in ambient air temperatures. Therefore, exceedance of T_{optA} by prevailing mean air temperatures across treatments implies that the frequent and severe heat stress predicted under climate change will further constrain carbon uptake in boreal forest conifers.

Until now, knowledge of the thermal acclimation of T_{optA} and its underlying processes was largely based on short-term studies with seedlings grown in artificial growth environments (e.g., pots) and in controlled environmental conditions (e.g., humidity, light). It was thus unclear whether those results would hold for mature trees growing in the field. Observed shifts in T_{optA} in our study are at the lower end of the spectrum (0.35–0.8 °C per 1 °C) reported for lab-based experimental studies with seedlings^{22, 30, 50}, but are comparable to mean values reported by recent meta-analyses for C₃ plants (0.34³¹ and 0.38¹¹ °C per 1 °C), indicating that while seedlings may have a greater ability to acclimate photosynthesis to warming than mature trees, average responses of photosynthetic thermal acclimation can be broadly used. Furthermore, the shift in T_{optA} with warming in our field study is much lower than that from a recent global compilation (0.62 °C per 1 °C) that estimated shifts in T_{optA} using seasonal changes in temperature (i.e., acclimatization). Therefore, we suggest that the use of temperature sensitivity parameters derived from ‘acclimatization studies’ should be used with caution when predicting the acclimation of forests to warming in global vegetation models. We also show that thermal acclimation of T_{optA} is strongly driven by concomitant adjustments of the thermal optima of photosynthetic biochemical processes (Fig. 2), and not changes in stomatal conductance or respiration (Supplementary Table 3a, b), findings that agree with prior work on controlled experiments in seedlings^{29, 30, 51}, field warming experiments^{19, 21, 52}, and a recent acclimatization study⁸. These results imply that changes in photosynthetic biochemical processes strongly underlie the adjustment of photosynthesis to long-term changes in growth temperature, regardless of experimental approach or tree life stage, although stomatal limitations are likely to play a greater role in limiting photosynthesis in water-stressed trees.

Most studies that have examined thermal acclimation of photosynthesis did so on ambient CO₂-grown trees. Elevated CO₂ is expected to influence the thermal acclimation of photosynthetic biochemistry (i.e., maximum Rubisco carboxylation rate, V_{cmax} , and maximum electron transport rates, J_{max}) mainly due to its suppressive effect on photorespiration^{53, 54} and its direct effects on Rubisco carboxylation^{35–37}, both of which are temperature dependent processes⁵. However, we show that elevated CO₂ does not largely affect the thermal optima or activation energies of V_{cmax} or J_{max} (Supplementary Fig. 3 and Supplementary Table 1). These findings with field-grown mature boreal trees agree with an earlier, short-term study with seedlings of the same species³⁰, suggesting that regardless of the experimental approach, life stage, and leaf habit, elevated CO₂ does not have strong effects on the thermal sensitivity of photosynthetic biochemical processes, such as V_{cmax} and J_{max} , in boreal conifers. Since V_{cmax} and J_{max} are key parameters for representing carbon uptake within TBMs⁶, our findings imply that potential interactive effects of elevated CO₂ on temperature sensitivity parameters of V_{cmax} and J_{max} (i.e., their activation energies and thermal optima) can be ignored in TBMs. Our findings also suggest that temperature response functions of these parameters, developed mainly from ambient CO₂-grown plants^{8, 46} and currently employed in all TBMs^{6, 7, 48} might accurately represent carbon uptake for trees growing in both current and projected elevated CO₂ conditions in future climates. However, further research on tree species from other biomes and plant functional types (e.g., broadleaved tree and shrub species) are still needed to validate this conclusion for broad use.

We show that the b parameter was generally increased by elevated CO₂ for both species, suggesting that elevated CO₂ increases the thermal sensitivity of net photosynthesis, a result in line with a shift to photosynthesis being more RuBP-regeneration limited at high CO₂ concentrations⁹. In addition, elevated CO₂ did affect the T_{optA} , but these effects were species dependent. In tamarack, the T_{optA} was higher in elevated CO₂, which likely reflects a direct suppression of photorespiration^{5, 9, 43, 54}. In contrast, there was no effect of elevated CO₂ on the T_{optA} in black spruce, and these results contrast prior findings in

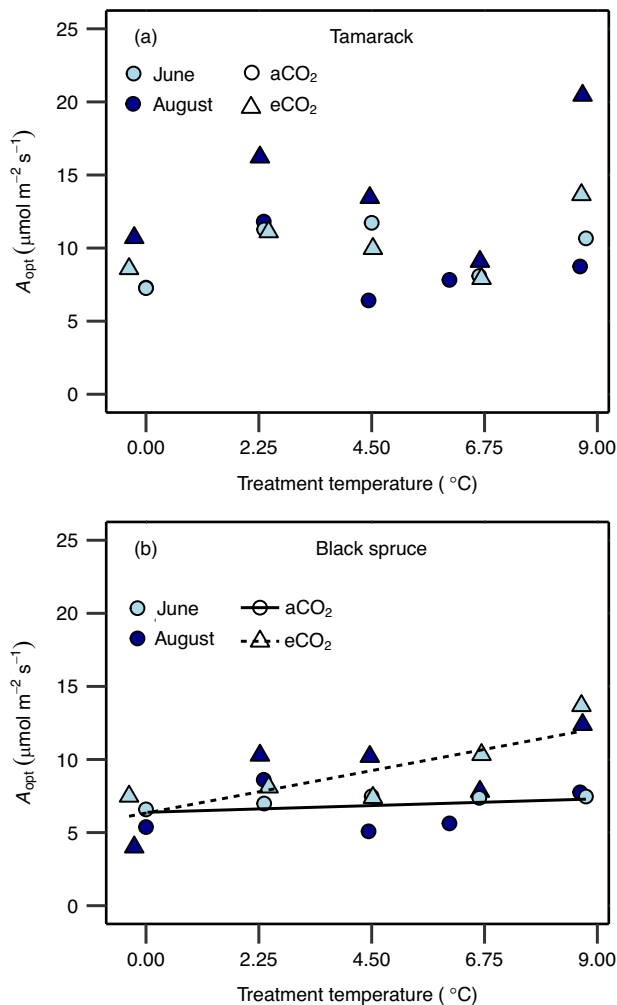


Fig. 4 | Net photosynthetic rates at the thermal optimum across warming and elevated CO₂ treatments. Impact of temperature and CO₂ treatments on net photosynthesis rate at the thermal optimum temperature (A_{opt}) in tamarack (a) and black spruce (b). The A_{opt} was estimated from temperature response of net photosynthesis measured at growth CO₂ using Eq. 2 (see “Methods”). Symbol colors represent the month in which measurements were taken (June = light blue; August = dark blue). Symbol shapes represent the CO₂ treatments (circle = ambient CO₂–aCO₂; triangles = elevated CO₂–eCO₂). A mixed-effects regression model was used to analyze the data where warming and elevated CO₂ treatment were the fixed effects, and the month in which the campaign was done was the random effect. The statistical test was one-sided since it was done to evaluate whether warming and elevated CO₂ stimulate A_{opt} . Lines in (b) represent regression lines: the solid ($y = 0.10x + 6.4$; $p = 0.54$) and the short-dashed ($y = 0.54x + 6.3$; $p = 0.029$) lines represent ambient and elevated CO₂, respectively. In (a), A_{opt} did not significantly change with treatments ($y = 0.26x + 7.9$, $p = 0.27$ and $y = 0.26x + 10.89$, $p = 0.27$, for ambient and elevated CO₂ treatments, respectively). Each data point represents the mean value of biologically independent trees measured in each plot ($n = 1\text{--}4$ trees/plot). Significance threshold: $p < 0.05$. Further details on statistical analyses for this figure can be found in Supplementary Table 1.

black spruce seedlings³⁰. The reasons behind this lack of elevated CO₂ effect on T_{optA} in mature black spruce are unclear since, similar to tamarack, the needle cohorts that were measured developed in prevailing environmental conditions across treatments. However, the magnitude of suppression of photorespiration by elevated CO₂ may vary across species or plant functional types—or in our case differences in leaf habit (evergreen versus deciduous). In our study, we cannot make a solid conclusion on the main cause for this, but two possibilities are differences in stomatal (Supplementary Fig. 13 and

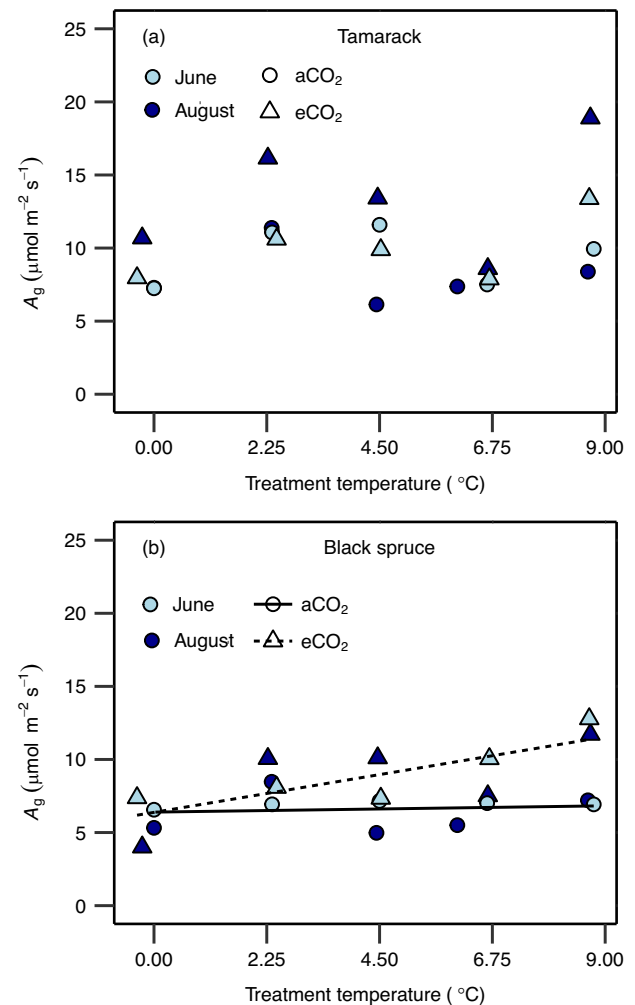


Fig. 5 | Net photosynthetic rates at prevailing growth temperatures across warming and elevated CO₂ treatments. Impact of temperature and CO₂ treatments on net photosynthesis rate estimated at mean growth temperature (9 a.m.–3 p.m.; A_g) in tamarack (a) and black spruce (b). Symbol colors represent the month in which measurements were taken (June = light blue; August = dark blue). Symbol shapes represent CO₂ treatments (circle = ambient CO₂–aCO₂; triangles = elevated CO₂–eCO₂). A mixed-effects regression model was used to analyze the data where warming and elevated CO₂ treatment were the fixed effects, and the month in which the campaign was done was the random effect. The statistical test was one-sided since it was done to evaluate whether warming and elevated CO₂ stimulate A_g . Lines in (b) represent regression lines: the solid ($y = 0.047x + 6.4$; $p = 0.76$) and the short-dashed ($y = 0.53x + 6.4$; $p = 0.026$) lines represent ambient and elevated CO₂, respectively. In (a), A_g did not significantly change with treatments ($y = 0.2x + 7.9$, $p = 0.35$ and $y = 0.2x + 10.79$, $p = 0.35$, for ambient and elevated CO₂ treatments, respectively). Each data point represents the mean value of biologically independent trees measured in each plot ($n = 1\text{--}4$ trees/plot). Significance threshold: $p < 0.05$. Further details on statistical analyses for this figure can be found in Supplementary Table 1.

Supplementary Table 1) and mesophyll conductance between the species. Our data shows little differences in intracellular CO₂ concentration between the two species across the two CO₂ treatments (Supplementary Fig. 14 and Supplementary Table 1), indicating that stomatal limitations are unlikely to underlie the difference in how T_{optA} responds to elevated CO₂. This leaves mesophyll conductance as a possible factor, as higher mesophyll conductance in tamarack could enhance CO₂ supply to Rubisco for a given unit of intercellular CO₂. However, without mesophyll conductance measurements we cannot directly prove this, and future research is needed to investigate this possibility.

Even though prevailing air temperatures largely exceeded T_{optA} , our findings show that photosynthesis acclimated such that at the prevailing daytime mean air temperature (between 9 a.m. and 3 p.m.), net carbon fixation remained constant or even increased (in eCO₂ black spruce trees) across the warming treatments (Fig. 5 and Supplementary Figs. 10 and 11). Therefore, our findings imply that warming alone may have little negative impacts on leaf-level carbon uptake in these cold-adapted mature boreal conifers when soil moisture is not limiting⁵⁵, as is the case at our current study site⁵⁶. However, ongoing climate change and the increased frequency of strong heat and dry spell events that will accompany it will likely reduce the ability of forests dominated by these species to fix and sequester carbon⁵⁷. Moreover, increased autotrophic respiration, which is temperature-dependent, has also been indicated as another factor that will release carbon sequestered in these North American boreal forests⁵⁸. Our previous work from this experiment support this, where we showed that foliar dark respiration did not thermally acclimate in these boreal conifers⁵⁶, suggesting that although carbon fixation may not be negatively impacted by warming, thermal effects on autotrophic respiration will further reduce the carbon sequestration potential of these forests⁵⁹.

In summary, our study has implications for the understanding of climate warming effects on carbon uptake of mature boreal conifers growing in field conditions, and for improving the representation of photosynthesis in TBMs. First, we show that although thermal acclimation of T_{optA} is limited and does not fully match increases in air temperature, photosynthetic carbon fixation is maintained at the prevailing growth conditions through a combination of photosynthetic acclimation and changes in instantaneous temperature responses of photosynthetic processes. Second, our study provides an improved framework for modeling photosynthesis in TBMs considering both warming and elevated CO₂, because we provide support for ignoring effects of elevated CO₂ on the thermal sensitivity of photosynthetic biochemical parameters (thermal optima and activation energies of V_{cmax} and J_{max})²². However, we show that it is important to account for effects of elevated CO₂ on the T_{optA} and on the overall thermal sensitivity of net photosynthesis (b parameter).

Methods

Site description and experimental design

This study was conducted at the Oak Ridge National Laboratory's SPRUCE (Spruce and Peatland Responses Under Changing Environments) project site at the U.S. Forest Service's Marcell Experimental Forest, in Minnesota, USA (47°30.476' N; 93°27.162' W). The details of the study site and experimental design are provided in recent studies from this experiment^{56,60–62}. But briefly, this forest grows naturally in a bog located at the southern limit of the boreal peatland forests. The forest is approximately 50 years old as it regenerated following canopy tree removal in 1969 and 1974⁶³. The dominant canopy species is *Picea mariana* (Mill.) B.S.P. (black spruce) mixed with less abundant *Larix laricina* (Du Roi) K. Koch (tamarack). The understory vegetation is dominated by ericaceous shrubs *Rhododendron groenlandicum* (Oeder) Kron & Judd and *Chamaedaphne calyculata* (L.) Moench. The experiment comprises five temperature treatments (ambient or +0, which serves also as the control, +2.25, +4.5, +6.75, and +9 °C above the ambient) established in a regression-based design⁶⁴. This experiment uses 10 large octagonal open-top enclosures with an interior surface area of 114.8 m², and a sampling area of 66.4 m². Five enclosures have an ambient-CO₂ atmosphere, while the other five have an elevated CO₂ atmosphere varying between +430 and 500 ppm above the ambient. The heating treatments started August 15, 2015, and CO₂ treatments were initiated a year later, on June 15, 2016. The targeted temperature treatments and CO₂ concentrations were largely achieved (Supplementary Fig. 12).

Plant material sampling and gas exchange measurements

Field measurements were conducted between June 18–30 and August 15–30, 2017. The daytime temperatures (4:00 a.m.–8:30 p.m.) during June and August were 18.97 and 18.02 °C, respectively. We studied the two mixed-age (up to ~45 years old) canopy tree species at SPRUCE, *Picea mariana* (Mill.) B.S.P. (black spruce) and *Larix laricina* (Du Roi) K. Koch (tamarack). For black spruce, one branchlet for each, randomly selected tree and in each plot was harvested and 1-year needle cohorts (i.e., developed in growth season of 2016) from each branch was measured. For tamarack, fully expanded current year foliage was used. In the June field campaign, three trees in each plot were randomly sampled, while in the August campaign, only two trees were used. For tamarack, we used the same number of branchlets from different trees in each plot, except in one plot (in ambient CO₂ and +0) where only one tamarack tree was available to be sampled. All measurements were made on sun-exposed branchlets cut using a pruning pole. After cutting, branchlets were put in water, and recut under water to avoid xylem transport disruption and stomatal closure. The branches were harvested between 4 and 5 a.m. of the measurement day, placed in water bottles inside a plastic cooler, and transported from the field site in Marcell, Minnesota to the walk-in growth chambers at the University of Minnesota in St. Paul, where the measurements were conducted. The branchlets were re-cut again before starting the measurements. The effect of cutting and the time lag between cutting and gas exchange measurements has been shown not to have significant effect on stomatal conductance in conifers⁶⁵. Gas exchange measurements were conducted between 10:00 and 20:00 using 7 portable photosynthesis systems (LI-COR 6400 XT, 6400-18 RGB light source, and 6400-22 opaque conifer chamber; LI-COR Biosciences, Lincoln, NE, USA). Net CO₂ assimilation rates (A) were measured at a pre-determined saturating light (1800 μmol m⁻² s⁻¹) and eleven different air CO₂ concentrations (to generate so-called $A-C_i$ curves) in the following order: 400, 300, 200, 50, 400, 500, 600, 800, 1200, 1600, and 2000 μmol mol⁻¹. The $A-C_i$ curves were conducted at five different leaf temperatures (T_{leaf}): 15, 25, 32.5, 40, and 45 °C. In order to achieve each targeted T_{leaf} , all measurements were completed inside the growth chamber, allowing the entire branch to be exposed to the desired temperature for at least 30 min before starting measurements at that temperature. As the gas exchange systems were also inside the chamber, this method minimized the measurement error driven by the internal thermal gradient that was recently reported for the LI-6400 instruments⁶⁶. Since the vapor pressure of the air (VPD_{air}) increases with increasing temperature, resulting in decreased stomatal conductance⁴⁵, we moistened the soda lime column of the gas exchange systems to reduce stomatal closure associated with high VPDs at high measurement temperatures (>32.5 °C). In total, we present results of 96 $A-C_i$ temperature response curves. After gas exchange measurements, projected leaf area of the measured needles was determined using ImageJ 1.51 software (NH, Bethesda, MD, USA). We, thereafter, corrected for the total leaf area before the analyses.

Parameterization

The FvCB (Farquhar, von Caemmerer, and Berry) C₃ photosynthesis model⁶⁷ was used to derive V_{cmax} and J_{max} from the $A-C_i$ curves using the fitacis function from the plantecophys 1.4-6 R package⁶⁸ and using the bilinear fitting method. We maintained the default temperature dependencies of the CO₂ compensation point in the absence of mitochondrial respiration (I^*) and the Michaelis–Menten constants for CO₂ and O₂ (K_c and K_o) from Bernacchi et al.⁶⁹. The leaf mesophyll conductance for CO₂ was not measured, therefore apparent V_{cmax} and J_{max} based on intercellular CO₂ concentrations (C_i), rather than the CO₂ concentration at the site of carboxylation (C_c) in the chloroplast, were estimated. The temperature sensitivity parameters of V_{cmax} (T_{optV} and E_{av}) and J_{max} (T_{optJ} and E_{aj}) were derived using the modified Arrhenius

function outlined in the following Eq. 1⁷⁰:

$$f(T_k) = k_{\text{opt}} \frac{H_d \exp\left(\frac{E_a(T_k - T_{\text{opt}})}{T_k R T_{\text{opt}}}\right)}{H_d - E_a \left(1 - \exp\left(\frac{H_d(T_k - T_{\text{opt}})}{T_k R T_{\text{opt}}}\right)\right)} \quad (1)$$

where k_{opt} is the process rate (i.e., V_{cmax} or J_{max} ; $\mu\text{mol m}^{-2} \text{s}^{-1}$) at the optimum temperature (V_{cmaxopt} , J_{maxopt}), H_d (kJ mol^{-1}) is the deactivation energy term that describes the decline in enzyme activity at higher temperature, E_a (kJ mol^{-1}) is the activation energy term that describes the exponential increase in enzyme activity with an increase in temperature, R is the universal gas constant ($8.314 \text{ J mol}^{-1} \text{ K}^{-1}$), and T_{opt} and T_k are the optimum and given temperatures of the process rate (i.e., V_{cmax} or J_{max} ; $\mu\text{mol m}^{-2} \text{s}^{-1}$). The value of H_d was fixed at 200 kJ mol^{-1} to avoid over-parameterization^{70,71}.

Net photosynthesis data at the tree growth CO_2 (400 or ~ 800 ppm, for ambient CO_2 and elevated CO_2 treatments, respectively) were extracted from the $A-C_i$ curves. Thereafter, the temperature response of A was fitted using the following Eq. 2¹⁶ to estimate the T_{optA} :

$$A(T) = A_{\text{opt}} - b(T - T_{\text{optA}})^2 \quad (2)$$

where $A(T)$ is the A ($\mu\text{mol m}^{-2} \text{s}^{-1}$) at a given air temperature T ($^{\circ}\text{C}$), A_{opt} is the A at the optimum temperature (T_{optA}), and the b parameter represents the breadth of the photosynthetic temperature response curve; larger values of b indicates that $A(T)$ has greater sensitivity to changes in T . After fitting b and T_{optA} , we used Eq. 2 to model net photosynthesis at prevailing growth temperature conditions using mean and maximum air temperature (9–4 a.m.) for each plot for 10 days preceding measurement of each tree/species, as well as for the entire growing season period (June–September) of both 2016 and 2017.

In order to estimate to what extent stomatal conductance may have affected the shifts in T_{optA} , we re-calculated net photosynthesis at a C_i/C_a ratio of 0.7 (A_{70} ; with a final C_i of 280 or 560 ppm for ambient and elevated CO_2 , respectively) using the parameterized V_{cmax} , J_{max} , R_{day} , and TPU (triose phosphate use) from the plantecophys 1.4-6 R package in the following equations⁴⁴:

$$A_c = \frac{V_{\text{cmax}}(C_i - \Gamma^*)}{[C_i + K_c(1 + \frac{O}{K_o})]} - R_{\text{day}} \quad (3)$$

where O the intercellular concentrations of O_2 , K_c and K_o are the Michaelis–Menten coefficients of Rubisco activity for CO_2 and O_2 , respectively, and Γ^* is the CO_2 compensation point in the absence of mitochondrial respiration. Values at 25°C and temperature sensitivities of Γ^* , K_c and K_o were taken from Bernacchi et al.⁶⁹.

$$A_j = \left(\frac{J_{\text{max}}}{4}\right) \times \frac{(C_i - \Gamma^*)}{(C_i + 2\Gamma^*)} - R_{\text{day}} \quad (4)$$

$$A_{\text{TPU}} = 3\text{TPU} \quad (5)$$

A_{70} was considered as the minimum of A_c , A_j , and A_{TPU} , and T_{optA} of A_{70} was estimated using Eq. 2.

Statistical tests. In order to evaluate the effect of elevated CO_2 on the thermal acclimation of the photosynthetic parameters, we used a mixed-effects regression model where warming and elevated CO_2 treatment were the fixed effects, and the month in which the campaign was done was the random effect. All analyses were run on the plot

means with $n=1-4$ trees/plot. The selection of the final statistical model was done in two steps following the protocol proposed by Zuur et al.⁷². We first evaluated whether a random factor was required by comparing the model with the random intercept (i.e., month) with the model without any random structure using the `gls` function of the `nlme` 3.1.162 R Package⁷³ and the method set to the Restricted maximum likelihood (REML). We did not include the model with a random slope and intercept structure since preliminary analyses indicated that the statistical model was over-parameterized. Thereafter, the model with the adequate random structure was selected based on the lowest AIC (Akaike Information Criterion) using the R `anova` function. After, the selection of the adequate random structure, we then selected for the adequate fixed effect structure between the structure with just main effects (i.e., warming and elevated CO_2) without interaction and with interaction. The latter selection was done by comparing these two fixed effect structures using the maximum likelihood–ML method within the `gls` function. Similarly, the best fixed effect structure was selected based on the lowest AIC value. But because our sample size is relatively small, we then computed the AICc using `AICmodavg` 2.3-2 R package⁷⁴ (Supplementary Tables 6 and 7). We also run ANOVA tests to examine the effects of temperature and elevated CO_2 treatments on delta-mean temperature growth (ΔMeanTg ; Supplementary Table 4). All analyses were conducted in R 3.6.1 software. (R Core Team, 2019), except for unpaired t Tests (Supplementary Table 3a, b) that were performed using statistical package in Excel 16.74 software.

Reporting summary

Further information on research design is available in the Nature Portfolio Reporting Summary linked to this article.

Data availability

The raw and processed (i.e., mean values used to generate each figure in the paper) photosynthesis data generated in this study have been deposited in the figshare database and can be accessed at <https://doi.org/10.6084/m9.figshare.22645030>⁷⁵. The complete leaf gas exchange data, including the data used in this paper, are also available through the SPRUCE project website at <https://doi.org/10.25581/spruce.056/1455138>⁷⁶.

Code availability

The R codes used for analyses for each figure included in this paper can be accessed at <https://doi.org/10.6084/m9.figshare.22645030>⁷⁵.

References

1. Friedlingstein, P. et al. Global carbon budget 2020. *Earth Syst. Sci. Data* **12**, 3269–3340 (2020).
2. Beer, C. et al. Terrestrial gross carbon dioxide uptake: global distribution and covariation with climate. *Science* **329**, 834–838 (2010).
3. Keenan, T. F. et al. Recent pause in the growth rate of atmospheric CO_2 due to enhanced terrestrial carbon uptake. *Nat. Commun.* **7**, 13428 (2016).
4. Chen, C., Riley, W. J., Prentice, I. C. & Keenan, T. F. CO_2 fertilization of terrestrial photosynthesis inferred from site to global scales. *Proc. Natl Acad. Sci. USA* **119**, e2115627119 (2022).
5. Dusenage, M. E., Duarte, A. G. & Way, D. A. Plant carbon metabolism and climate change: elevated CO_2 and temperature impacts on photosynthesis, photorespiration and respiration. *N. Phytol.* **221**, 32–49 (2019).
6. Mercado, L. M. et al. Large sensitivity in land carbon storage due to geographical and temporal variation in the thermal response of photosynthetic capacity. *N. Phytol.* **218**, 1462–1477 (2018).
7. Oliver, R. J. et al. Improved representation of plant physiology in the JULES-vn5.6 land surface model: Photosynthesis, stomatal

- conductance and thermal acclimation. *Geosci. Model Dev.* **15**, 5567–5592 (2022).
8. Kumarathunge, D. P. et al. Acclimation and adaptation components of the temperature dependence of plant photosynthesis at the global scale. *N. Phytol.* **222**, 768–784 (2019).
 9. Sage, R. F. & Kubien, D. S. The temperature response of C₃ and C₄ photosynthesis. *Plant Cell Environ.* **30**, 1086–1106 (2007).
 10. Way, D. A. Just the right temperature. *Nat. Ecol. Evol.* **3**, 718–719 (2019).
 11. Yamori, W., Hikosaka, K. & Way, D. A. Temperature response of photosynthesis in C₃, C₄, and CAM plants: temperature acclimation and temperature adaptation. *Photosynth. Res.* **119**, 101–117 (2014).
 12. Los, D. A. & Murata, N. Membrane fluidity and its roles in the perception of environmental signals. *Biochim. Biophys. Acta* **1666**, 142–157 (2004).
 13. Murakami, Y., Tsuyama, M., Kobayashi, Y., Kodama, H. & Iba, K. Trienoic fatty acids and plant tolerance of high temperature. *Science* **287**, 476–479 (2000).
 14. Gu, L. et al. An exploratory steady-state redox model of photosynthetic linear electron transport for use in complete modelling of photosynthesis for broad applications. *Plant Cell Environ.* **46**, 1540–1561 (2023).
 15. Lin, Y.-S., Medlyn, B. E. & Ellsworth, D. S. Temperature responses of leaf net photosynthesis: the role of component processes. *Tree Physiol.* **32**, 219–231 (2012).
 16. Scafaro, A. P., Posch, B. C., Evans, J. R., Farquhar, G. D. & Atkin, O. K. Rubisco deactivation and chloroplast electron transport rates co-limit photosynthesis above optimal leaf temperature in terrestrial plants. *Nat. Commun.* **14**, 2820 (2023).
 17. Way, D. A. & Yamori, W. Thermal acclimation of photosynthesis: on the importance of adjusting our definitions and accounting for thermal acclimation of respiration. *Photosynth. Res.* **119**, 89–100 (2014).
 18. Berry, J. & Bjorkman, O. Photosynthetic response and adaptation to temperature in higher plants. *Annu. Rev. Plant Physiol.* **31**, 491–543 (1980).
 19. Sendall, K. M. et al. Acclimation of photosynthetic temperature optima of temperate and boreal tree species in response to experimental forest warming. *Glob. Chang. Biol.* **21**, 1342–1357 (2015).
 20. Smith, N. G. & Dukes, J. S. Short-term acclimation to warmer temperatures accelerates leaf carbon exchange processes across plant types. *Glob. Chang. Biol.* **23**, 4840–4853 (2017).
 21. Gunderson, C. A., O'Hara, K. H., Campion, C. M., Walker, A. V. & Edwards, N. T. Thermal plasticity of photosynthesis: the role of acclimation in forest responses to a warming climate. *Glob. Chang. Biol.* **16**, 2272–2286 (2009).
 22. Choury, Z. et al. Tropical rainforest species have larger increases in temperature optima with warming than warm-temperate rainforest trees. *N. Phytol.* **234**, 1220–1236 (2022).
 23. Crous, K. Y. et al. Photosynthesis of temperate *Eucalyptus globulus* trees outside their native range has limited adjustment to elevated CO₂ and climate warming. *Glob. Chang. Biol.* **19**, 3790–3807 (2013).
 24. Wittermann, M. et al. Temperature acclimation of net photosynthesis and its underlying component processes in four tropical tree species. *Tree Physiol.* **42**, 1188–1202 (2022).
 25. Cavanagh, A. P., Slattery, R. & Kubien, D. S. Temperature induced changes in Arabidopsis Rubisco activity and isoform expression. *J. Exp. Bot.* **74**, 651–663 (2022).
 26. Slot, M. & Kitajima, K. General patterns of acclimation of leaf respiration to elevated temperatures across biomes and plant types. *Oecologia* **177**, 885–900 (2015).
 27. Mujawamariya, M. et al. Complete or overcompensatory thermal acclimation of leaf dark respiration in African tropical trees. *N. Phytol.* **229**, 2548–2561 (2021).
 28. Atkin, O. K. & Tjoelker, M. G. Thermal acclimation and the dynamic response of plant respiration to temperature. *Trends Plant Sci.* **8**, 343–351 (2003).
 29. Dusenage, M. E. et al. Limited thermal acclimation of photosynthesis in tropical montane tree species. *Glob. Chang. Biol.* **27**, 4860–4878 (2021).
 30. Dusenage, M. E., Madhavji, S. & Way, D. A. Contrasting acclimation responses to elevated CO₂ and warming between an evergreen and a deciduous boreal conifer. *Glob. Chang. Biol.* **26**, 3639–3657 (2020).
 31. Crous, K. Y., Uddling, J. & De Kauwe, M. G. Temperature responses of photosynthesis and respiration in evergreen trees from boreal to tropical latitudes. *N. Phytol.* **234**, 353–374 (2022).
 32. Way, D. A. & Sage, R. F. Thermal acclimation of photosynthesis in black spruce [*Picea mariana* (Mill.) B.S.P.]. *Plant Cell Environ.* **31**, 1250–1262 (2008).
 33. Zhang, X. W. et al. Higher thermal acclimation potential of respiration but not photosynthesis in two alpine *Picea* taxa in contrast to two lowland congeners. *PLoS ONE* **10**, e0123248 (2015).
 34. Kurepin, L. V. et al. Contrasting acclimation abilities of two dominant boreal conifers to elevated CO₂ and temperature. *Plant Cell Environ.* **41**, 1331–1345 (2018).
 35. Ainsworth, E. A. & Long, S. P. What have we learned from 15 years of free-air CO₂ enrichment (FACE)? A meta-analytic review of the responses of photosynthesis, canopy properties and plant production to rising CO₂. *N. Phytol.* **165**, 351–371 (2005).
 36. Leakey, A. D. B. et al. Elevated CO₂ effects on plant carbon, nitrogen, and water relations: six important lessons from FACE. *J. Exp. Bot.* **60**, 2859–2876 (2009).
 37. Gardner, A., Ellsworth, D. S., Crous, K. Y., Pritchard, J. & MacKenzie, A. R. Is photosynthetic enhancement sustained through three years of elevated CO₂ exposure in 175-year-old *Quercus robur*? *Tree Physiol.* **42**, 130–144 (2022).
 38. Pastore, M. A., Lee, T. D., Hobbie, S. E. & Reich, P. B. Strong photosynthetic acclimation and enhanced water-use efficiency in grassland functional groups persist over 21 years of CO₂ enrichment, independent of nitrogen supply. *Glob. Chang. Biol.* **25**, 3031–304 (2019).
 39. Norby, R. J., Warren, J. M., Iversen, C. M., Medlyn, B. E. & McMurtrie, R. E. CO₂ enhancement of forest productivity constrained by limited nitrogen availability. *Proc. Natl Acad. Sci. USA* **107**, 19368–19373 (2010).
 40. Moore, B. D., Cheng, S. H., Sims, D. & Seemann, J. R. The biochemical and molecular basis for photosynthetic acclimation to elevated atmospheric CO₂. *Plant Cell Environ.* **22**, 567–582 (1999).
 41. Medlyn, B. E. et al. Effects of elevated [CO₂] on photosynthesis in European forest species: a meta-analysis of model parameters. *Plant Cell Environ.* **22**, 1475–1495 (1999).
 42. Warren, J. M., Jensen, A. M., Medlyn, B. E., Norby, R. J. & Tissue, D. T. Carbon dioxide stimulation of photosynthesis in *Liquidambar styraciflua* is not sustained during a 12-year field experiment. *AoB Plants* **7**, plu074 (2014).
 43. Wujeska-Klaue, A., Crous, K. Y., Ghannoum, O. & Ellsworth, D. S. Lower photorespiration in elevated CO₂ reduces leaf N concentrations in mature *Eucalyptus* trees in the field. *Glob. Chang. Biol.* **25**, 1282–1295 (2019).
 44. von Caemmerer, S. *Biochemical Models of Leaf Photosynthesis* (CSIRO Publishing, 2000).
 45. Šigut, L. et al. Does long-term cultivation of saplings under elevated CO₂ concentration influence their photosynthetic response to temperature? *Ann. Bot.* **116**, 929–939 (2015).
 46. Kattge, J. & Knorr, W. Temperature acclimation in a biochemical model of photosynthesis: a reanalysis of data from 36 species. *Plant Cell Environ.* **30**, 1176–1190 (2007).

47. Way, D. A., Oren, R. & Kroner, Y. The space-time continuum: the effects of elevated CO₂ and temperature on trees and the importance of scaling. *Plant Cell Environ.* **38**, 991–1007 (2015).
48. Smith, N. G., Malyshev, S. L., Shevliakova, E., Kattge, J. & Dukes, J. S. Foliar temperature acclimation reduces simulated carbon sensitivity to climate. *Nat. Clim. Chang.* **6**, 407–411 (2015).
49. Blonder, B. & Michaletz, S. T. A model for leaf temperature decoupling from air temperature. *Agric. For. Meteorol.* **262**, 354–360 (2018).
50. Slot, M. & Winter, K. Photosynthetic acclimation to warming in tropical forest tree seedlings. *J. Exp. Bot.* **68**, 2275–2284 (2017).
51. Yamaguchi, D. P. et al. Limitation in the photosynthetic acclimation to high temperature in canopy leaves of *Quercus serrata*. *Front. For. Glob. Chang.* <https://doi.org/10.3389/ffgc.2019.00019> (2019).
52. Stefanski, A., Bermudez, R., Sendall, K. M., Montgomery, R. A. & Reich, P. B. Surprising lack of sensitivity of biochemical limitation of photosynthesis of nine tree species to open-air experimental warming and reduced rainfall in a southern boreal forest. *Glob. Chang. Biol.* **26**, 746–759 (2019).
53. Smith, N. G. & Keenan, T. F. Mechanisms underlying leaf photosynthetic acclimation to warming and elevated CO₂ as inferred from least-cost optimality theory. *Glob. Chang. Biol.* **26**, 5202–5216 (2020).
54. Long, S. P. Modification of the response of photosynthetic productivity to rising temperature by atmospheric CO₂ concentrations: has its importance been underestimated? *Plant Cell Environ.* **4**, 729–739 (1991).
55. Reich, P. B. et al. Effects of climate warming on photosynthesis in boreal tree species depend on soil moisture. *Nature* **562**, 263–267 (2018).
56. Dusenage, M. E. et al. Warming induces divergent stomatal dynamics in co-occurring boreal trees. *Glob. Chang. Biol.* **27**, 3079–3094 (2021).
57. Girardin, M. P. et al. Negative impacts of high temperatures on growth of black spruce forests intensify with the anticipated climate warming. *Glob. Chang. Biol.* **22**, 627–643 (2016).
58. Reich, P. B. et al. Boreal and temperate trees show strong acclimation of respiration to warming. *Nature* **531**, 633–636 (2016).
59. Marchand, W., Girardin, M. P., Hartmann, H., Gauthier, S. & Bergeron, Y. Taxonomy, together with ontogeny and growing conditions, drives needleleaf species' sensitivity to climate in boreal North America. *Glob. Chang. Biol.* **25**, 2793–2809 (2019).
60. Richardson, A. D. et al. Ecosystem warming extends vegetation activity but heightens vulnerability to cold temperatures. *Nature* **560**, 368–371 (2018).
61. Malhotra, A. et al. Peatland warming strongly increases fine-root growth. *Proc. Natl Acad. Sci. USA* **117**, 17627–17634 (2020).
62. Ward, E. J. et al. Photosynthetic and respiratory responses of two bog shrub species to whole ecosystem warming and elevated CO₂ at the boreal-temperate ecotone. *Front. For. Glob. Chang.* <https://doi.org/10.3389/ffgc.2019.00054> (2019).
63. Sebestyen, S. et al. in *Peatland Biogeochemistry and Watershed Hydrology at the Marcell Experimental Forest* (ed. Brooks, K.) 15–71 (CRC Press, 2011).
64. Hanson, P. J. et al. Attaining whole-ecosystem warming using air and deep-soil heating methods with an elevated CO₂ atmosphere. *Biogeosciences* **14**, 861–883 (2017).
65. Akalusi, M. E., Meng, F. R. & P-A Bourque, C. Photosynthetic parameters and stomatal conductance in attached and detached balsam fir foliage. *Plant Environ. Interact.* **2**, 206–215 (2021).
66. Garen, J. C. et al. Gas exchange analysers exhibit large measurement error driven by internal thermal gradients. *N. Phytol.* **236**, 369–384 (2022).
67. Farquhar, G. D., von Caemmerer, S. & Berry, J. A. A biochemical model of photosynthetic CO₂ assimilation in leaves of C₃ species. *Planta* **149**, 78–90 (1980).
68. Duursma, R. A. & Plantecophys-An, R. Package for analysing and modelling leaf gas exchange data. *PLoS ONE* **10**, e0143346 (2015).
69. Bernacchi, C. J., Singaas, E. L., Pimentel, C., Portis, A. R. Jr & Long, S. P. Improved temperature response functions for models of Rubisco-limited photosynthesis. *Plant Cell Environ.* **24**, 253–259 (2001).
70. Medlyn, B. E. et al. Temperature response of parameters of a biochemically based model of photosynthesis. II. A review of experimental data. *Plant Cell Environ.* **25**, 1167–1179 (2002).
71. Dreyer, E., Le Roux, X., Montpied, P., Daudet, F. A. & Masson, F. Temperature response of leaf photosynthetic capacity in seedlings from seven temperate tree species. *Tree Physiol.* **21**, 223–232 (2001).
72. Zuur, A. F., Ieno, E. N., Walker, N., Saveliev, A. A. & Smith, G. M. *Mixed Effects Models and Extensions in Ecology with R* (Springer New York, 2009).
73. Pinheiro, J., Bates, D. & R Core Team. nlme: Linear and nonlinear mixed effects models. R package version 3.1-162. <https://CRAN.R-project.org/package=nlme> (2023).
74. Mazerolle, M. J. AICcmodavg: model selection and multimodel inference based on (Q)AIC(c). R package version 2.3.2. <https://cran.r-project.org/package=AICcmodavg> (2023).
75. Dusenage, M. E. et al. Dataset and R codes for the article: Boreal conifers maintain carbon uptake with warming despite failure to track optimal temperatures. figshare <https://doi.org/10.6084/m9.figshare.22645030> (2023).
76. Dusenage, M. E. et al. SPRUCE photosynthesis and respiration of *Picea mariana* and *Larix laricina* in SPRUCE experimental plots, 2016–2017. Oak Ridge National Laboratory (ORNL), Oak Ridge, TN (United States). <https://doi.org/10.25581/spruce.056/1455138> (2020).

Acknowledgements

Research was sponsored by the Biological and Environmental Research Program in the Office of Science, U.S. Department of Energy managed by UT- Battelle, LLC, for the U.S. Department of Energy under contract DEAC05-00OR22725. M.E.D., J.M.W., E.J.W., D.A.M., A.W.K. and P.J.H. were supported under this contract. E.J.W. also acknowledges support from USGS Climate Research and Development Program. P.B.R., A.S., R.B., and R.A.M acknowledge funding support by the U.S. NSF Biological Integration Institutes grant DBI-2021898. D.A.W. acknowledges funding from the NSERC Discovery and Strategic programs (RGPIN/04677-2019 and STPGP/521445-2018), the Research School of Biology at the Australian National University, and the U.S. Department of Energy contract No. DE-SC0012704 to Brookhaven National Laboratory. Notice: This manuscript has been authored by UT-Battelle, LLC, under contract DE-AC05-00OR22725 with the US Department of Energy (DOE). The US government retains and the publisher, by accepting the article for publication, acknowledges that the US government retains a non-exclusive, paid-up, irrevocable, worldwide license to publish or reproduce the published form of this manuscript, or allow others to do so, for US government purposes. DOE will provide public access to these results of federally sponsored research in accordance with the DOE Public Access Plan (<http://energy.gov/downloads/doe-public-access-plan>). The DOI link for the dataset used in this paper can be accessed at <https://doi.org/10.25581/spruce.056/1455138> and <https://doi.org/10.6084/m9.figshare.22645030>. Any use of trade, firm, or product names is for descriptive purposes only and does not imply endorsement by the U.S. Government.

Author contributions

M.E.D., J.M.W., E.J.W., P.J.H., and D.A.W. designed the research; M.E.D., J.M.W., E.J.W., B.K.M., A.S., R.B., M.C., D.A.M., and A.W.K. collected the data; M.E.D. analyzed the data; M.E.D. wrote the manuscript with significant contributions from J.M.W., P.B.R., and D.A.W.; E.J.W., B.K.M., A.S., R.B., M.C., D.A.M., A.W.K., R.A.M., and P.J.H. provided editorial advice. All co-authors commented on versions of the manuscript.

Competing interests

The authors declare no competing interests.

Additional information

Supplementary information The online version contains supplementary material available at <https://doi.org/10.1038/s41467-023-40248-3>.

Correspondence and requests for materials should be addressed to Mirindi Eric Dusenge or Danielle A. Way.

Peer review information *Nature Communications* thanks Bradley Posch and the other, anonymous, reviewer(s) for their contribution to the peer review of this work. A peer review file is available.

Reprints and permissions information is available at <http://www.nature.com/reprints>

Publisher's note Springer Nature remains neutral with regard to jurisdictional claims in published maps and institutional affiliations.

Open Access This article is licensed under a Creative Commons Attribution 4.0 International License, which permits use, sharing, adaptation, distribution and reproduction in any medium or format, as long as you give appropriate credit to the original author(s) and the source, provide a link to the Creative Commons licence, and indicate if changes were made. The images or other third party material in this article are included in the article's Creative Commons licence, unless indicated otherwise in a credit line to the material. If material is not included in the article's Creative Commons licence and your intended use is not permitted by statutory regulation or exceeds the permitted use, you will need to obtain permission directly from the copyright holder. To view a copy of this licence, visit <http://creativecommons.org/licenses/by/4.0/>.

© The Author(s) 2023